How Long Cylindrical Micelles Formed after Extruding Block Copolymer in a Selective Solvent through a Small Pore Fragment back into Spherical Ones

ARTICLE *in* MACROMOLECULES · NOVEMBER 2013

Impact Factor: 5.8 · DOI: 10.1021/ma4016449

3 AUTHORS:

Qianjin Chen
University of Utah
19 PUBLICATIONS **163** CITATIONS
SEE PROFILE

Yuan Li
The Chinese University of Hong Kong
3 PUBLICATIONS **9** CITATIONS
SEE PROFILE

Chi yo wu
The Chinese University of Hong Kong
240 PUBLICATIONS **7,222** CITATIONS
SEE PROFILE

Macromolecules

Note

pubs.acs.org/Macromolecules

How Long Cylindrical Micelles Formed after Extruding Block Copolymer in a Selective Solvent through a Small Pore Fragment back into Spherical Ones

Qianjin Chen,[†,*] Yuan Li,[†,*] and Chi Wu[†,‡]

[†]Department of Chemistry, The Chinese University of Hong Kong, Shatin, N.T., Hong Kong

[‡]The Hefei National Laboratory of Physical Science at Microscale, Department of Chemical Physics, The University of Science and Technology of China, Hefei, Anhui 230026, China

Supporting Information

ABSTRACT: The slow cylinder-to-sphere transition for cylindrical micelles from nanopore extrusion is quantitatively investigated by using transmission electron microscopy. The time-dependent length distribution and weight-average length of cylindrical micelles from experiment were compared with those calculated ones from computer simulation on the basis of end-scission, random-scission and Gaussian-scission models. The results reveal that the cylinder-to-sphere transition involves a combination of the Gaussian-scission model and the end-scission model and the scission rate constant is nearly a linear function of micelle length but slightly increases with time for a given length. As expected, such a thermal agitation induced transition with the spherical phase as its thermodynamically stable state is different from those previously observed in the shear-induced fragmentation of long cylindrical micelles made of amphiphilic block copolymers in a selective solvent.

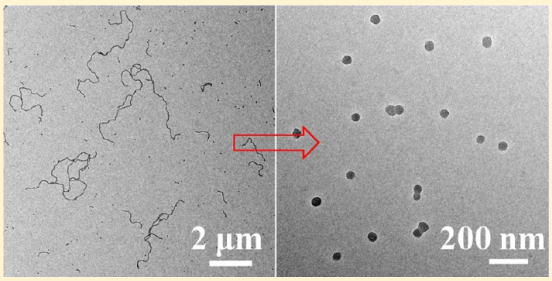

It has been known that amphiphilic block copolymer chains in a selective solvent can assemble into thermodynamically stable spherical or cylindrical micelles or aggregates into kinetically controlled vesicle-like, toroidal and multicompartment micellar structures,[1−3] depending on their molecular structures. These colloids have a range of potential applications such as catalyst support and drug delivery carrier. Because of each specific application requires specially designed structure, the control of those micelle morphologies becomes very important. In general, it has been realized by adjusting the composition of block copolymers,[4,5] polymer concentration,[6] solvent composition,[7] and temperature[8] or by adding different amounts of homopolymer of the insoluble block.[9] Understanding the micelle morphology transition from one into another can help explore desirable nanostructures and their further applications.

While many studies on these micelle morphology transitions were only phenomenal, the detailed transition kinetics and mechanism were also revealed, but still qualitative.[10,11] Therefore, further quantitative studies are necessary to elicit the transition mechanisms, especially between spheres and cylinders. Previously, we found a novel sphere-to-cylinder transition induced by extruding a dispersion of spherical micelles made of diblock copolymer through a small cylindrical pore in a properly chosen solvent mixture.[12] It is found that such obtained cylindrical micelles were very slowly fragmenting into individual spherical micelles, since the worm-like cylindrical micelles are only kinetically trapped while the spherical micelles are thermodynamically favored. Such a cylinder-to-sphere transition in the dispersions after the extrusion lasted from minutes to weeks, depending on the dispersion conditions. In the current study, we quantitatively studied this slow cylinder-to-sphere transition by using a combination of experimental and simulated results.

The long cylindrical micelles are prepared from extrusion of small spherical micelles made of diblock copolymer polystyrene-*b*-polyisoprene (PS_{285}-*b*-PI_{245}) in a mixture solvent of THF and *n*-hexane (13:87, v/v%) through small cylindrical nanopores ($d \sim 20$ nm). The TEM in Figure 1 and Figure S1 (Supporting Information) show that besides those long cylindrical micelles with a diameter of ∼40 nm and a length over micrometers, there are also many small spherical and short cylindrical micelles in the dispersion. Length of those cylindrical micelles was measured over many TEM images. We only analysis those cylindrical micelles with a length longer than 400 nm, i.e., those made of 10 or more spherical micelles, since small spheres and short cylinders can potentially influence our statistical analysis. Such a procedure is also applied to the time dependent TEM analysis and further computer simulation. Both the number and weight distribution ($f_n(L)$ and $f_w(L)$) of cylindrical micelle length are broad, as indicated in Figure 1, and $f_n(L)$ highlights shorter cylinders with a peak at ∼0.7−0.8 μm.

Received: August 6, 2013
Revised: October 23, 2013

   dx.doi.org/10.1021/ma4016449 | *Macromolecules* XXXX, XXX, XXX−XXX

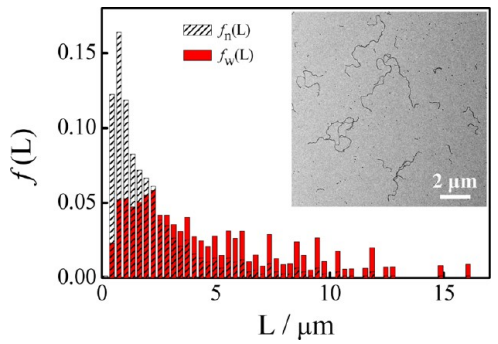

Figure 1. TEM image and characterization of number and weight distribution of cylindrical micelle length just after their formation.

Further TEM images of cylindrical micelles at different time in the dispersion during the cylinder-to-sphere transition are presented in Figure 2. Compared with Figure 1, the average length of cylindrical micelles becomes shorter and more spherical micelles are visible. After two weeks, only spherical micelles are observed in the TEM images. Using these TEM images, we characterized time-dependent $f_n(L)$ and $f_w(L)$ of cylindrical micelle length and calculated the number- and weight-average lengths (L_n and L_w) of cylindrical micelles at different dissociation times, as summarized in Table S1 (Supporting Information) and plotted in Figure 3. The L_w for cylindrical micelles just after extrusion is ~4.6 μm, quite consistent with the value 4.7 ± 0.1 μm deduced from LLS measurements using the Holter-Casassa analysis (Figure S2 and S3, Supporting Information); and L_w decreases gradually due to the cylinder-to-sphere transition.

Our cylinder-to-sphere transition is parallel to polymer chain degradation if we regard each long cylindrical micelle is made of many small spherical units that are temporarily connected by sufficiently strong physical interaction, while in a polymer chain monomers are linked together by much stronger chemical bonds. On the basis of previous works on polymer chains degradation under sonication using computer simulation,[13,14] here, we applied three different fundamental "scission" models including the end-scission, random-scission and Gaussian-scission to study the fragmentation of long cylindrical micelles. Each cylindrical micelle with a length L_i (made of i spherical micelles, subunits) can split into two shorter ones with j and $i-j$ subunits with a scission rate constant k_{ij}. Further assumptions and definition of these models are provided in the Supporting Information.

With the experimentally determined initial length distribution, we simulated the cylinder-to-sphere transition by using the above three scission models and calculated the time-dependent L_w, as shown in Figure 3. It is clear that the simulated and measured L_w have a similar relaxation behavior. Note that X and Y account for the length and time dependences, respectively, and R defines the location range of the scission site along a given cylindrical micelle. The best fittings of our experimentally measured L_w lead to Y = 0.5 for end-scission model; X = 0.9 and Y = 0.2 for random-scission model; and X = 0.9, Y = 0.2, and R = 0.35 for Gaussian-scission model. Figure 3 shows that both the random and Gaussian scission models agree with the experimental results well but not the end-scission model.

Experimental results showed that the population of spherical micelles in the TEM images steadily increased with the time and nearly all cylindrical micelles were fragmented into

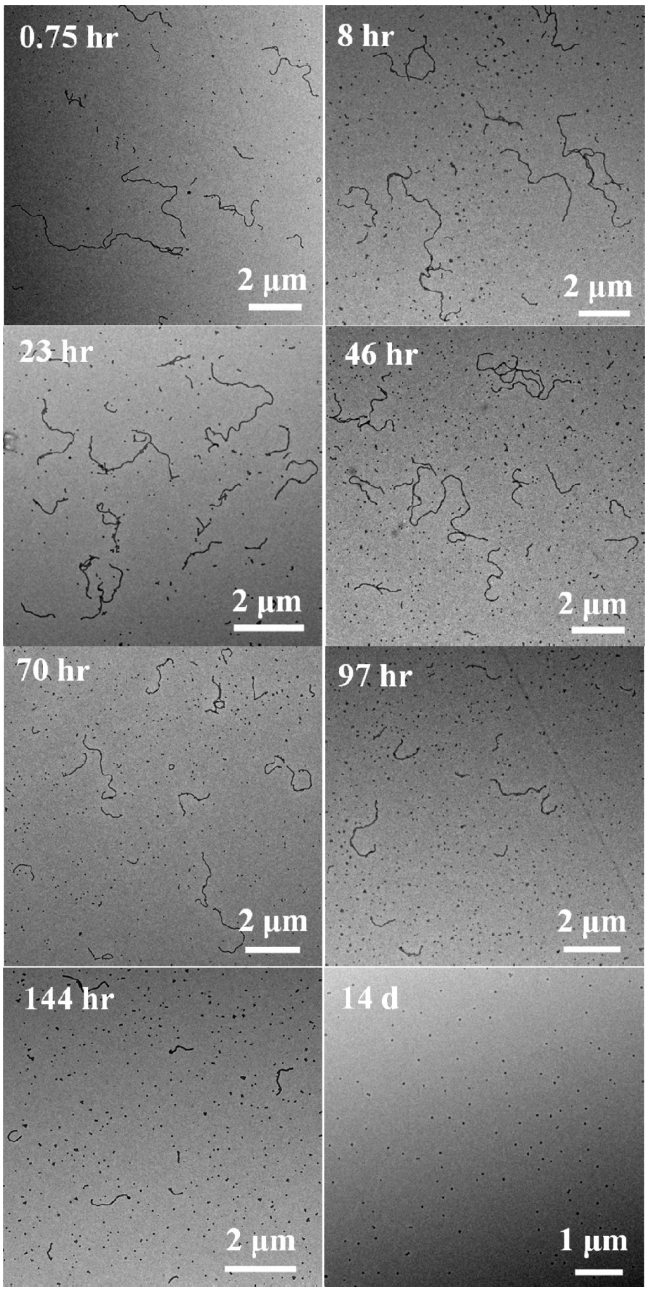

Figure 2. TEM images of cylindrical micelles during cylinder-to-sphere transition.

spherical micelles at the end, which cannot be explained by either the random or Gaussian scission model. Actually, each cylindrical micelle could be treated as a string of partially interconnected "pearls" (spherical micelles), presumably due to the compression and forced fusion of small spherical micelles inside the long cylindrical pore during formation. If only considering the surface tension, each spherical micelle would tend to break off at the ends of a cylindrical micelle, similar to the Rayleigh instability description.[15] On the other hand, if considering a cylindrical micelle as a breakable chain, a simple calculation of its length-dependent configuration entropy change indicates that it prefers a scission in the middle. On the basis of above considerations, a new complex scission model that combines the Gaussian- and end-scissions, wherein the scission probability at the two ends is higher; while that at

dx.doi.org/10.1021/ma4016449 | *Macromolecules* XXXX, XXX, XXX–XXX

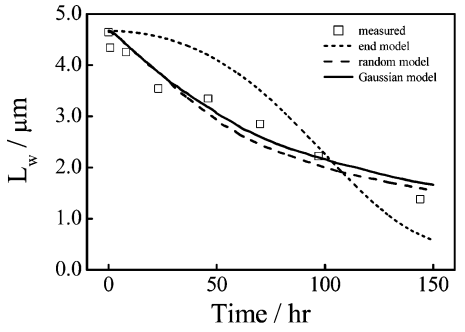

Figure 3. Time dependence of experimental and simulated L_w of cylindrical micelles during cylinder-to-sphere transition by using end-scission model ($Y = 0.5$), random-scission model ($X = 0.9$ and $Y = 0.2$) and Gaussian-scission model ($X = 0.9$, $Y = 0.2$, and $R = 0.35$), where time is measured with Monte Carlo cycles by same ratio.

other places follows the Gaussian distribution is proposed. A parameter of p is introduced to weight the end scission probability. Therefore, the reaction rate constant of the jth subunit along a cylindrical micelle is expressed by a piecewise function as

$$k_{ij} = \begin{cases} pk_0(i-1)^X t^Y, & \text{if } j = 1 \text{ or } i-1 \\ k_0(i-1)^X t^Y \dfrac{1}{\sigma_j\sqrt{2\pi}} \exp\left[-\left(j - \dfrac{i}{2}\right)^2 / 2\sigma_j^2\right], & \\ \text{otherwise} & \end{cases} \quad (1)$$

The simulation results in $f_w(L)$ of cylindrical micelle length and its corresponding L_w. Figure 4 shows that the simulated and measured $f_w(L)$ agree well with each other when $p = 20$ is used, i.e., if the end scission has 3 k_BT free energy preference. The

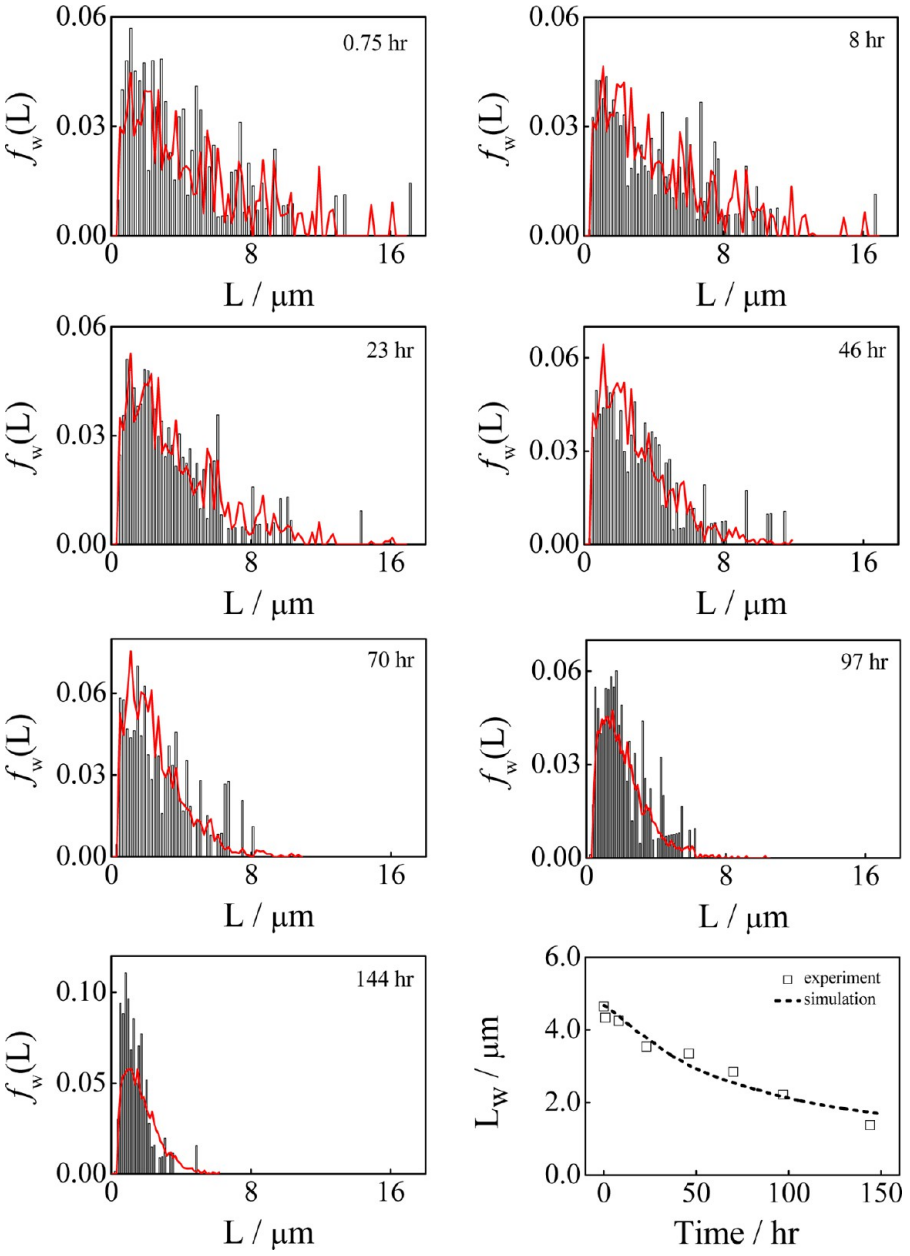

Figure 4. Time dependence of weight distribution cylindrical micelle length, where black bars: TEM results; red curves: simulation results, and bottom right figure compares calculated and measured L_w with best fitting parameters ($X = 0.9$, $Y = 0.2$, $R = 0.35$, and $p = 20$).

dx.doi.org/10.1021/ma4016449 | *Macromolecules* XXXX, XXX, XXX–XXX

value of $X = 0.9$ reflects that the scission rate constant is nearly a linear function of the micelle length, consistent with previous studies of polymer degradation; and the positive value of $Y = 0.2$ reveals that the scission rate constant slightly increases with time, different from the fragmentation of cylindrical micelles under a shear force. Such a time dependent scission rate constant might be explained as follows. The thermal fluctuation agitates each cylindrical micelle to move in the dispersion and constantly change its conformation to create some kinks and defects between two fused and adjacent spherical micelles. The thermal agitation of shorter cylinders should be easier than that of long ones, causing more kinks and defects per unit length for shorter cylinders. As the fragmentation proceeds, each cylindrical micelle becomes shorter and the overall scission rate becomes faster.

In conclusion, the slow cylinder-to-sphere transition agitated by thermal fluctuation for cylindrical micelles from nanopore extrusion is quantitatively studied. A comparison of measured and simulated weight-average length and length distribution and discussions of the thermodynamics for the phase transition reveal that the transition kinetics is governed by a model that combines both the Gaussian-scission model with its highest scission probability located in the middle of a cylinder and the end-scission model with scission probability at the two ends of a cylinder. The scission rate constant is nearly proportional to the micelle length and slightly increases with the time. We can conclude that the scission mechanism of long cylindrical micelles formed from nanopore extrusion is different from those previously observed under an external shear force for long cylindrical micelles formed via the self-assembly of amphiphilic block copolymers in a selective solvent, where the thermodynamically stable state is the cylindrical phase.[16]

■ ASSOCIATED CONTENT

Ⓢ Supporting Information

Detailed experimental section, TEM images for cylindrical micelles after extrusion, laser light scattering characterization and computer simulation for the cylinder-to-sphere transition, etc. This material is available free of charge via the Internet at http://pubs.acs.org.

■ AUTHOR INFORMATION

Corresponding Author

*E-mail: (Q.C.) qianjin5100@hotmail.com; (Y.L.) frogly@126.com).

Notes

The authors declare no competing financial interest.

■ ACKNOWLEDGMENTS

The financial support of the National Natural Scientific Foundation of China Projects (20934005 and 51173177), the Ministry of Science and Technology of China Key Project (2012CB933802), and the Hong Kong Special Administration Region Earmarked Projects (CUHK4042/10P, 2130241; 2060405; CUHK4036/11P, 2130281; 2060431, and CUHK7/CRF/12G) is gratefully acknowledged.

■ REFERENCES

(1) Lazzari, M.; Liu, G.; Lecommandoux, S. *Block Copolymers in Nanoscience*; Wiley-VCH: New York, 2006.
(2) Jain, S.; Bates, F. S. *Science* **2003**, *300*, 460.
(3) Moughton, A. O.; Hillmyer, M. A.; Lodge, T. P. *Macromolecules* **2012**, *45*, 2.
(4) Zhang, L.; Eisenberg, A. *Science* **1995**, *268*, 1728.
(5) Zhang, L. F.; Eisenberg, A. *J. Am. Chem. Soc.* **1996**, *118*, 3168.
(6) Zhang, L. F.; Eisenberg, A. *Macromolecules* **1999**, *32*, 2239.
(7) Bang, J.; Jain, S.; Li, Z.; Lodge, T. P.; Pedersen, J. S.; Kesselman, E.; Talmon, Y. *Macromolecules* **2006**, *39*, 1199.
(8) Bhargava, P.; Tu, Y.; Zheng, J. X.; Xiong, H.; Quirk, R. P.; Cheng, S. Z. D. *J. Am. Chem. Soc.* **2007**, *129*, 1113.
(9) Ouarti, N.; Viville, P.; Lazzaroni, R.; Minatti, E.; Schappacher, M.; Deffieux, A.; Borsali, R. *Langmuir* **2005**, *21*, 1180.
(10) Burke, S. E.; Eisenberg, A. *Langmuir* **2001**, *17*, 6705.
(11) Denkova, A. G.; Mendes, E.; Coppens, M. O. *J. Phys. Chem. B* **2009**, *113*, 989.
(12) Chen, Q.; Zhao, H.; Ming, T.; Wang, J.; Wu, C. *J. Am. Chem. Soc.* **2009**, *131*, 16650.
(13) Ballauff, M.; Wolf, B. A. *Macromolecules* **1981**, *14*, 654.
(14) Tanigawa, M.; Suzuto, M.; Fukudome, K.; Yamaoka, K. *Macromolecules* **1996**, *29*, 7418.
(15) Fan, P. W.; Chen, W. L.; Lee, T. H.; Chiu, Y. J.; Chen, J. T. *Macromolecules* **2012**, *45*, 5816.
(16) Guerin, G.; Wang, H.; Manners, I.; Winnik, M. A. *J. Am. Chem. Soc.* **2008**, *130*, 14763.